

**AUDITORY BRAIN STEM RESPONSES IN THE CAT. I. INTRACRANIAL AND EXTRACRANIAL RECORDINGS**<sup>1,2</sup>L. JOSEPH ACHOR and ARNOLD STARR<sup>3</sup>*Departments of Psychobiology and Neurology, University of California at Irvine, Irvine, Calif. 92717 (U.S.A.)*

(Accepted for publication: May 21, 1979)

The early portion of the scalp-recorded auditory evoked potential in the cat consists of 5 or 6 major peaks with a latency of less than 6 msec (Fig. 1, top trace) and is called the auditory brain stem response (ABR). The generators for several of the peaks of the ABR have been attributed to specific portions of the brain stem auditory pathway on the basis of (1) latency correlations between surface- and depth-recorded activity (Jewett 1970; Lev and Sohmer 1972), and (2) changes in the ABR as a result of transecting the brain stem at various levels of the auditory pathway (Buchwald and Huang 1975; Goldenberg and Derbyshire 1975). The results of these studies suggest that the principal generators for the peaks of the ABR are: peak 1, eighth nerve; peak 2, cochlear nucleus; peak 3, the region of the superior olivary complex; peak 4, the region of the lateral lemniscus and/or inferior colliculus; and peak 5, the region of the lateral lemniscus and/or inferior colliculus. The results of the lesion study by Buchwald

and Huang (1975) also suggested that the first two components are generated prior to any decussation of the auditory pathway, components 3 and 5 are largely dependent upon the integrity of crossed projections and component 4 is dependent upon both crossed and uncrossed projections.

While it is well-known that there is considerable temporal overlap in the activity occurring in the various brain stem auditory structures (Jungert 1958; Wicklegren 1968), the studies above suggest that at the latencies corresponding to each of the peaks of the ABR the activity in a single site is substantially greater than anywhere else in the brain stem. As a similar (though perhaps not identical) sequence of potentials is recorded in man and used in neurological diagnosis (Starr and Achor 1975; Thornton and Hawkes 1976; Stockard and Rossiter 1977), the definition of the generators in the cat may aid in the analysis of the generation of the ABR in man.

In the present study all of the sites of substantial brain stem activity were defined for each of the peaks and troughs of the ABR. The basic latency correlation between depth- and surface-recorded activity used by Jewett (1970) and Lev and Sohmer (1972) was extended to a multiplanar 2-dimensional spatial analysis of the voltage fields as a function of time. This analysis permitted a more detailed specification of the magnitude, polarity, spatial extent and temporal development of the voltage fields in the brain stem. Although several factors (e.g., open versus

<sup>1</sup> This work was submitted by L.J. Achor in partial fulfillment of the requirements for the degree Doctor of Philosophy, Department of Psychobiology, University of California, Irvine.

<sup>2</sup> This research was supported by Research Grants NS-10399 and NS-11876 from the National Institutes of Health to A. Starr. L.J. Achor was supported by NIMH Training Grants MH11095 and 1 T32 MH14599, by an NIMH predoctoral fellowship 5 FO 1 MH58170 and by an award from the Chancellor's Patent Fund, University of California, Irvine.

<sup>3</sup> To whom reprint requests should be addressed.

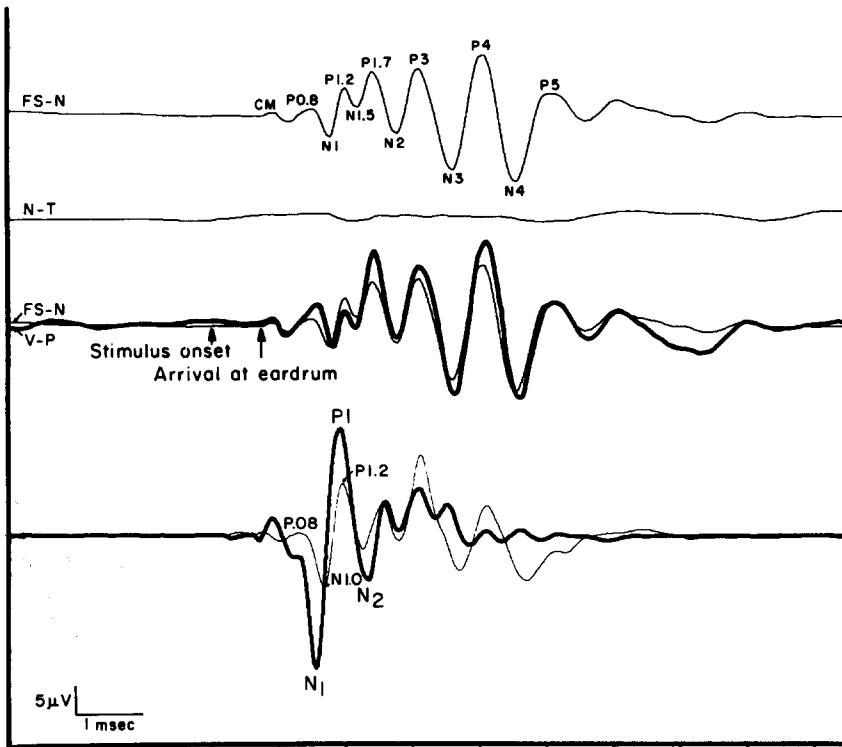


Fig. 1. Auditory evoked potentials obtained with various recording configurations. The top record (labeled FS-N) is the ABR recorded in the cat from the frontal sinus referenced to the neck. Each positive-going peak or negative-going trough has been designated with the letter P or N, respectively, and with a number which identifies the latency of the component from the time of arrival of the stimulus at the eardrum under standard conditions (94 dB SPL peak equivalent click, 25/sec stimulus rate, barbiturate anesthesia). In this and all subsequent figures of the ABR, positivity at the screw electrode in the frontal sinus is displayed upwards. Each trace is the average of 100 responses to a click stimulus presented at 25/sec. CM indicates the beginning of cochlear microphonic activity. The second trace is the auditory evoked potential obtained with the configuration neck referenced to tail (N-T). The third and fourth (overlapped) traces are recordings obtained from the frontal sinus referenced to the neck (FS-N, thin trace) and vertex referenced to pinna (V-P, thick trace). The bottom pair of traces are the frontal sinus referenced to the neck (thin trace) and the round window response referenced to the neck (thick trace). Components P0.8, N1.0 and P1.2 of the ABR occur at the same time as components N1-P1 of the round window recording. The amplitude calibration is  $5 \mu\text{V}$  for all of the records except the round window recording which has a calibration of  $50 \mu\text{V}$ .

closed fields, inhomogeneities of the brain and geometry of the neural generators) limit the latency correlation technique, it was our judgment that this approach was a useful method of analysis for studying the generation of the surface-recorded evoked responses. In an accompanying paper (Achor and Starr, 1980) the effects of discrete brain stem lesions in cats on the components of the ABR are presented.

## Methods

### Subjects

Of 19 adult cats studied, 4 were selected for analysis. The others were eliminated from consideration because of (1) a change of 10% or more in the amplitude of one or more of the components during the recording session, (2) incomplete spatial sampling of the brain

stem, or (3) deficiencies in the histological reconstruction of the electrode tracks. Although some damage to the brain was expected with the multiple electrode penetrations, it was assumed that the damage was negligible if the amplitudes of the components of the ABR remained unchanged during the recording session.

### *Surgery*

The cats were anesthetized with 40 mg/kg sodium pentobarbital administered intraperitoneally. In several pilot experiments it was found that following the administration of sodium pentobarbital there were small changes in the ABR. In comparison with the ABR from the unanesthetized cat the amplitudes of the components were reduced by 5–10% and the latencies of the components beginning with P4 were increased by 50–150  $\mu$ sec.

Following anesthesia the animal was placed in a stereotaxic frame with hollow ear bars. A bilateral craniotomy was performed anterior and posterior to the tentorium exposing the cortex and cerebellum. The dura was removed and the exposed brain kept moist with warm saline-soaked pads. Rectal temperature was maintained at 36–38°C by means of a circulating water pad. Anesthesia was maintained with supplemental doses of sodium pentobarbital.

### *Stimulus generation*

Monaural 'click' stimuli (produced by a shielded Beyer transducer, energized by a 100  $\mu$ sec square wave pulse) were presented at 25/sec. The changes which occurred in the ABR as a function of increasing the stimulus rate from the conventional 10/sec to the 25/sec used in the present study were limited to increases in latency for components P4, N4 and P5 of less than 100  $\mu$ sec and decreases in amplitude of less than 10% for these same components. A 3.5 cm length of polyethylene tubing, containing fine steel wool for acoustic

damping, was interposed between the transducer and the hollow ear bar. The acoustic stimulus was calibrated with a sound level meter in a soft-walled coupler. A short length of polyethylene tubing was used to provide an 0.1 ml cavity between the tip of the hollow ear bar and the sound level meter equipped with a 0.25 in. condenser microphone. The output voltage of the sound level meter in response to the condensation click stimulus is shown in Fig. 2A. The intensity of the click was 94 dB SPL peak equivalent with a background of 57 dB SPL. The spectral energy of the click was broadly distributed below 4 kHz and was maximal about 1 kHz (Fig. 2B). The click stimulus was 65 dB above threshold for a jury of 3 normal hearing adult human subjects. The stimulus level used for each of the animal subjects was selected on the basis of providing distinct wave forms on the linear portion of the ABR latency-intensity function. The input voltages to the transducer used for cats 1, 2, 3 and 4 were -20 dB, 0 dB, -10 dB, and 0 dB (*re.* 94 dB SPL peak equivalent), respectively.

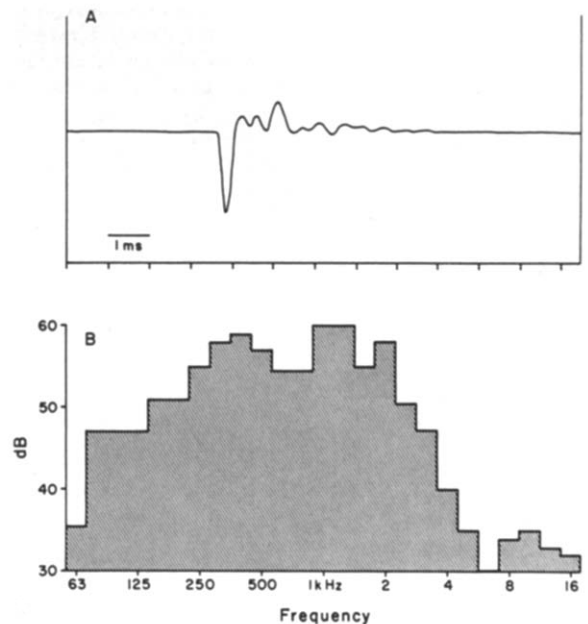


Fig. 2. The acoustic wave form of the click stimulus (A) and the spectral energy in dB SPL (B).

### *Recording*

The ABR was recorded between a screw placed in the frontal sinus 1 cm anterior to the intersection of the coronal and mid-sagittal sutures and a reference electrode clipped to the skin at the midline of the base of the neck. The neck was chosen as the site for the reference electrode because there was minimal activity in neck referenced to tail recordings (N-T in Fig. 1). The frontal sinus was used as the 'active' electrode because the bilateral craniotomy left only a tiny isthmus of bone at the conventional vertex site. For comparison an ABR recorded from the conventional configuration vertex referenced to pinna (thick trace, V-P) has been overlaid on the ABR recorded from the frontal sinus referenced to the neck (thin trace, FS-N) in Fig. 1. The latencies of the components of the ABR obtained from the vertex referenced to the pinna were the same as those obtained from the frontal sinus referenced to the neck, but the amplitudes of the components differed. In the vertex referenced to pinna recording all of the components, except P1.2, N2.0 and P5 were slightly larger. Component P1.2 in some of the cats in this study was minimal or absent in vertex referenced to pinna recordings, as in the studies by Buchwald and Huang (1975), Berry et al. (1976), Jewett (1970) and Lev and Sohmer (1972).

Depth recordings were obtained from a 125  $\mu\text{m}$  diameter insulated tungsten electrode referenced to the neck. The tip was beveled at 75° by a rotating abrasive stone. Battery-operated amplifiers located inside the acoustic room amplified the depth activity 1000 times and the ABR 10,000 times. The bandpass was 100 Hz–3 kHz (–6 dB points, 12 dB/octave) for both the ABR and depth recordings for cats 1 and 2 and 1 Hz–10 kHz for cats 3 and 4. The amplified signals were led to a PDP 11/40 computer and monitored on an oscilloscope. Positivity at the screw electrode (relative to the neck reference) for the ABR and at the tungsten electrode for the depth activity was displayed in an upwards direction. The

evoked activity was sampled at a rate of 40 kHz (25  $\mu\text{sec}$  bin width) and averaged over 100 trials. The analysis epoch of 12.80 msec (512 points) consisted of a 3.00 msec pre-stimulus period and a 9.80 msec post-stimulus period. The digitized data were stored on magnetic disks for subsequent analysis.

### *Recording sequence*

An acoustic intensity series was run for each ear at the beginning of the recording session for each animal. Frequently, differences in ABR threshold of 20 dB or more were observed between the two ears. The ear with the lowest ABR threshold was designated as the stimulus ear and the experimental protocol were begun.

Approximately 40 penetrations were made into the brain of each animal, with each electrode penetration being preceded by a surface recording. It was necessary to monitor the ABR in this manner, because the latencies of the components changed over the long recording sessions (minimum of 8 h) as shown in Fig. 3. The latency changes were related to alterations in body temperature as previously reported by Williston and Jewett (1977) and to depth of anesthesia. Recordings were obtained from the brain stem and from regions of the cerebellum and cortex in the paths of the electrode penetrations. The stereotaxic coordinates for each recording site were chosen to maximize the total area of the brain stem sampled, while maintaining a simple spatial relationship between the recording points to facilitate computer analysis. The angled entry of the penetrations (30° from the vertical) enabled sampling of portions of the auditory pathway adjacent to the bony tentorium. The two groups of penetrations (pre- and post-tentorium) formed a 'V' in sagittal view (Fig. 4). Penetrations were made in 9 parasagittal planes separated from one another by 2 mm (C8, C6, C4, 0, I2, I4, I6, I8 (C = contralateral, I = ipsilateral)). Stereotaxic zero was a line parallel and 10 mm dorsal to the interaural line. The horizontal spacing

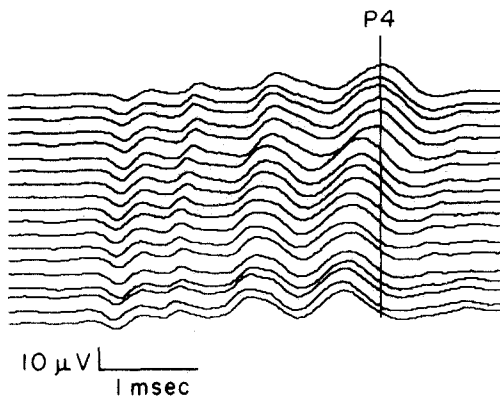


Fig. 3. Latency changes in the ABR during a recording session. This figure contains a sequence of ABRs (recorded from the frontal sinus referenced to the neck) obtained over a period of 9 h. In this figure the click occurs at the onset of the trace. The vertical line is aligned at the latency of component P4 of the ABR recorded at the beginning of the recording session (top trace). During the recording session the latencies of all of the components of the ABR in this animal became shorter. The progressive latency decrements were correlated with a gradual small rise in body temperature.

between rows of penetrations, the lateral spacing between each parasagittal plane of penetrations and the distance between recording sites along a given penetration were arranged so that the intended placement of each recording point was 2 mm from adjacent points. The 2 mm grid provided the most favorable trade-off between (1) the needed spatial sampling and (2) the adverse effects of excessively large numbers of penetrations and/or long hours of recording. Applying sample theory (Brigham 1974) to spatial frequency, the smallest separation of sites which can be discriminated using a 2 mm spatial sampling is 4 mm. The spatial separation of the nuclear auditory pathway was equal to or greater than 4 mm, but the separation of the fiber tracts from the adjacent nuclear structures of the auditory pathway was usually less. Thus, there were occasions when a given field could not be clearly associated with one

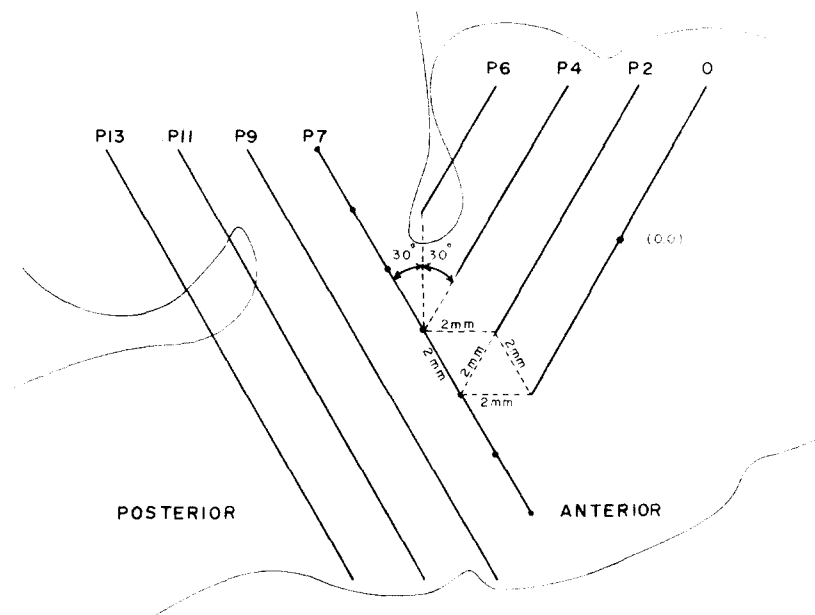


Fig. 4. Spatial pattern of recording sites. The spatial pattern of electrode tracks and recording sites is superimposed on the outline of a sagittal section of the brain stem at lateral 4. Four of the electrode paths (P13—P7) are angled forward and 4 (P6—P0) are angled backward. The 2 mm spacing of recording sites along a track is depicted for penetration 7. The spatial relationship of the two sets of angled penetrations is delineated in the center of the figure. Stereotaxic zero is at (0,0) along penetration P0. Penetrations were made in 9 parasagittal planes separated from one another by 2 mm (see Fig. 6).

or another structure. Two assumptions were utilized to improve the spatial resolution of the generator sites. First, the range of voltage values between any two adjacent recording sites were assumed to be within the voltage values at these two sites. Second, the decay of voltage with distance was assumed to be linear. These assumptions enabled the interpolation of imaginary data.

#### *Perfusion and histology*

Following testing, the animal was deeply anesthetized and then perfused through the heart with normal saline followed by 10% buffered formalin. The entire brain was removed, blocked and stored in 10% formalin for 1 week prior to processing.

Parasagittal serial sections (80  $\mu\text{m}$ ) were obtained by either frozen or rapid celloidin techniques. As an aid to track reconstruction, photographs were made of those (unstained) sections having electrode tracks. The photographs were enlarged by an appropriate factor for each animal to compensate for the tissue shrinkage. Shrinkage of the tissue during preparation was determined from the measured spacing between four or more adjacent electrode tracks in a given tissue section. Shrinkage was minimal for the tissue prepared by the frozen technique, but was approximately 20% for the tissue prepared by the rapid celloidin technique. For each animal, 9 representative anatomical reconstructions were made, corresponding to the 9 parasagittal planes of electrode penetrations. The electrode tracks in each of the 9 parasagittal planes were reconstructed from the photographs and superimposed on the appropriate histological reconstructions.

In several pilot experiments a small lesion was placed at the end of each of the 40 penetrations to facilitate histological reconstruction of the tracks and recording sites. These lesions markedly affected the ABR in terms of amplitude, latency and/or number of components. Thus, lesions were not made in the actual experiments and instead the electrode

tracks and recording sites were reconstructed on the basis of close inspection of the photographs for evidence of the passage of the electrode in the tissue. Error in specification of the end point of each electrode penetration by this technique was determined in pilot experiments to be a maximum of 0.5 mm. This determination was made on the basis of a comparison of end points of adjacent electrode penetrations at the same depth with and without marker lesions.

#### *Data analysis*

The data were analyzed using computer programs which permitted: subtraction of the pre-stimulus baseline activity; digital filtering; determination of the peak and trough latencies; and storage and scanning of a 4-dimensional representation of selected data (voltage as a function of time along the 3 spatial dimensions of rostral-caudal, medial-lateral, and dorsal-ventral).

The baseline subtraction program averaged the amplitude of the first 100 digitized points (2.5 msec) of the pre-stimulus baseline and subtracted this value from the entire wave form to compensate for any random slow potential shifts and/or amplifier DC bias that may have been present in the evoked potentials.

The ABR in man and other species has been customarily recorded with the amplifier bandpass set to attenuate low frequency electroencephalographic activity; however, a wide range of high-pass settings have been used from 10 Hz (Jewett and Williston 1971) to 500 Hz (Terkildsen et al. 1973). Although it was well-known that such differences in high-pass filtering could produce large changes in the evoked potentials recorded directly from the brain stem auditory structures, the change in the ABR was found to be limited to the elimination of a slow rise in the baseline. In order to assess the effects of filtering of the evoked activity on both the ABR and the distribution of the brain stem potentials, the data from cats 3 and 4 were collected with

the amplifier bandpass wide open (1 Hz–10 kHz) and then processed in 2 ways: (1) unfiltered, and (2) after digital filtering. In the digital filtering condition the bandpass was 160 Hz–3 kHz with essentially no roll-off or phase shifting. The potentials recorded from the surface and depth electrodes were filtered identically.

The latency values of the peaks and troughs of the surface-recorded ABR were obtained with the graphics display of the computer and retained for use in the following operation; for each peak or trough in the skull recording a 4-dimensional array of data from the brain stem was generated, which mapped voltage as a function of time in the 3 spatial dimensions of rostral-caudal, medial-lateral and dorsal-ventral at 3 instants of time: 100  $\mu$ sec before the component of the ABR attained its maximum amplitude, at the latency that the component attained its maximum amplitude, and 100  $\mu$ sec after the component attained its maximum amplitude. Then the absolute latencies were replaced with the generic terms: -100, peak or trough, +100. Thus, the absolute latency associated with a given peak on one penetration might be different from the absolute latency associated with this same peak on another penetration. This generic labeling provided the required flexibility in the latency correlation between the ABR and the depth activity to account for the body temperature related latency changes which occurred in the ABR wave form during the long recording sessions (see Fig. 3).

The data were printed on a teleprinter with one data sheet for each of the 9 parasagittal planes of section for each instant of time selected. The 2-dimensional array of voltage values on each data sheet spatially duplicated the separation of recording points in a given sagittal plane.

Each of the data sheets was overlaid by a photocopy of the appropriate plane of histological section and an isopotential map was then constructed by connecting the points having equal voltage. Adjustments were made, as necessary, for the deviation of the elec-

trode penetrations from their intended placements. Voltage values were linearly interpolated between real data points, an arbitrary approximation of actual voltage changes over distance. Isopotential lines were made by connecting points having equal voltage. The points at which there was no voltage difference between the depth and reference electrodes comprised the zero isopotential line. Positive and negative isopotential lines were drawn every 200  $\mu$ V beginning at the zero isopotential line to improve the visual display of voltage changes over distance. (As it is not possible to prove that the neck is at absolute zero, even by recordings referenced to the tail, positive and negative are only relative terms.) The isopotential maps were evaluated for the magnitude and polarity of the fields and for movement of the fields. Movement was inferred when there was a shift in the distribution of the field which occurred without any apparent change in magnitude.

## Results

### *Correlation of spatial and temporal distributions of evoked potentials in the brain stem and the scalp-recorded ABR*

The field maps for a given instant of time and plane of section were often quite similar across the 4 cats. This was particularly true for the components up to P3. However, for the later components (N3, P4 and N4), the data were less consistent. For example, at the latency of component P4 all of the 4 cats had a dipole field in the region of the ipsilateral superior olive. But in one animal the negative pole was much larger, in another the positive pole was much larger and in the other two the poles were approximately equal. As space limitations preclude the presentation of all of the idiosyncratic findings, data from just one of the cats will be described in detail. A summary of the data for the 4 animals is given in Fig. 15. The auditory structures in each of the reconstructed parasagittal planes for cat 4 are

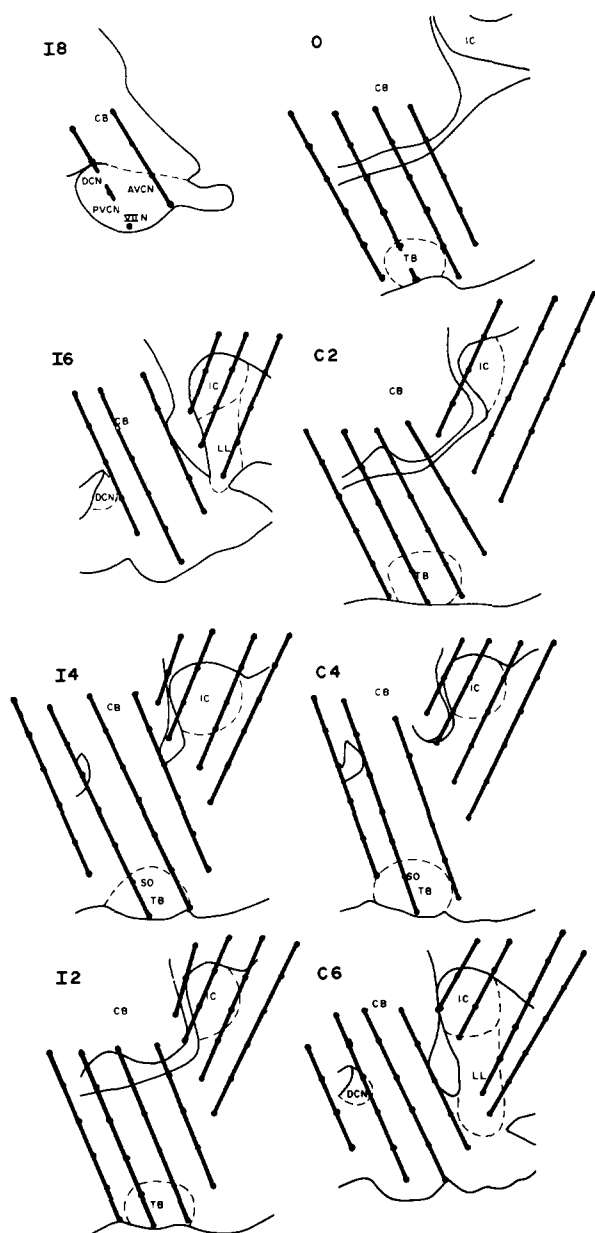


Fig. 5. Reconstructed parasagittal planes for cat 4. Each of the individual figures (I8, I6, I4, I2, O, C2, C4, C6) is representative of the anatomy for a set of penetrations at a given laterality (see Fig. 4). The letters I and C indicate ipsilateral and contralateral, respectively, and the numbers designate the stereotaxic plane of intended electrode entry. The rostral portion of each of the sections is to the right. No figure was made for C8 as there was little activity recorded in this region. The approximate extent of the auditory structures is given by the dashed lines.

labeled in Fig. 5. The plane of section containing the contralateral cochlear nucleus (plane C8) is not included as only minimal activity (less than  $200 \mu\text{V}$ ) was recorded in this region. The evoked potentials from this animal were collected without filtering (band-pass 1 Hz–10 kHz) and were then processed in two ways: unfiltered and after digital filtering. The field distributions derived from the unfiltered wave forms will be described first.

At the latencies corresponding to components P0.8, N1.0, P1.2 and N1.5 activity (i.e. a large positive or negative voltage difference between the depth electrode and the reference electrode at the neck) was recorded only from the electrode sites in the cochlear nucleus. Fig. 6 depicts the voltage fields in the cochlear nucleus at the latency of each of these components, as well as  $100 \mu\text{sec}$  before ( $-100$ ) and  $100 \mu\text{sec}$  after ( $+100$ ) each component.

#### P0.8

At the latency of component P0.8 there was a positive field near the site of entry of the eighth nerve in the midventral region of the cochlear nucleus. As the field was less than  $200 \mu\text{V}$  in amplitude, no isopotential lines are shown in the P0.8 portion of the figure.

#### N1.0

At  $100 \mu\text{sec}$  before the latency of component N1.0 the positive field in the cochlear nucleus had increased to  $400 \mu\text{V}$ . The maximum field recorded was located in the midventral region of the cochlear nucleus. By  $100 \mu\text{sec}$  after the latency of N1.0 the field had increased to  $1000 \mu\text{V}$  and shifted rostral and dorsal into the region of the anteroventral cochlear nucleus.

The small dots indicate the actual recording sites in cat 4. DCN, dorsal cochlear nucleus; PVCN, posteroventral cochlear nucleus; AVCN, anteroventral cochlear nucleus; VIII N., eighth nerve; CB, cerebellum; SO, superior olive; TB, trapezoid body; IC, inferior colliculus; LL, lateral lemniscus.

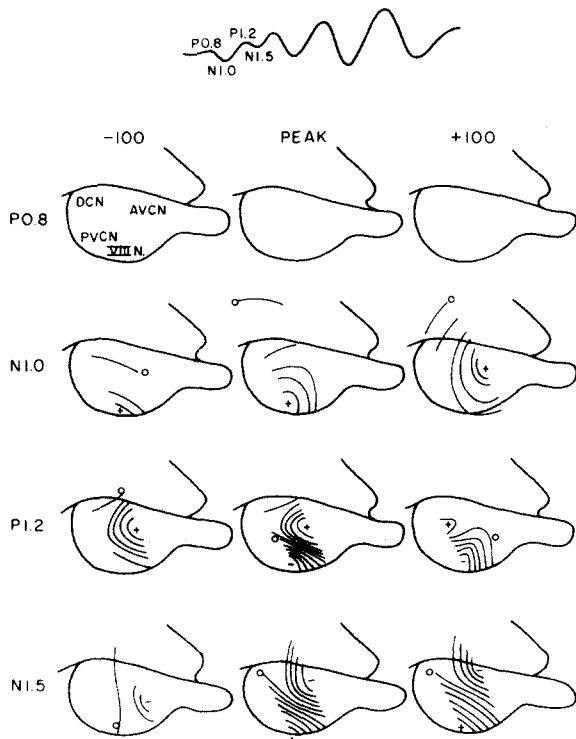


Fig. 6. Temporal development of the voltage fields in the cochlear nucleus at the times corresponding to components P0.8, N1.0, P1.2 and N1.5 of the ABR. The temporal development of the voltage fields in the cochlear nucleus can be seen in (a) the progressive changes in the field plots for each component (viewed from left to right), and (b) the changes in the field plots across components (viewed from top to bottom). The temporal development of brain stem activity at the latency of each component is characterized by 3 field plots, which represent 100  $\mu$ sec before the maximum of the component (labeled as -100), at the maximum of the component (labeled as peak) and 100  $\mu$ sec after the maximum of the component (labeled as +100). In this figure and in all other figures of the voltage fields, each of the isopotential lines on either side of the zero isopotential represent a change of 200  $\mu$ V. The activity was recorded with an amplifier bandpass of 1 Hz–10 kHz. The scalp derived ABR is at the top of the figure labeled with the components illustrated below. The labels in the upper left hand figure indicate eighth nerve (VIII N.), posteroventral cochlear nucleus (PVCN), anteroventral cochlear nucleus (AVCN), and dorsal cochlear nucleus (DCN). Note that the fields arise in the region of the entry of the eighth nerve into the cochlear nucleus and then shift anterodorsal into the region of the anteroventral cochlear nucleus.

### P1.2

At the latency of P1.2 a 1000  $\mu$ V negative field appeared in the midventral cochlear nucleus. The positive field located rostral and dorsal diminished to 200  $\mu$ V at 100  $\mu$ sec after P1.2.

### N1.5

At the latency of N1.5 the field in the cochlear nucleus reversed from the field seen at the latency of P1.2. An 800  $\mu$ V negative field was located rostral and dorsal in the region of the anteroventral cochlear nucleus and a 1200  $\mu$ V positive field was located in the midventral region of the cochlear nucleus near the site of entry of the eighth nerve.

### P1.7

At the latency of P1.7 (Fig. 7) the negative field in the cochlear nucleus diminished to 400  $\mu$ V and the positive field diminished to 600  $\mu$ V. Simultaneously, a positive field ranging from 200 to 600  $\mu$ V in amplitude developed from ipsilateral 4 to contralateral 4 in the ventral brain stem area (i.e., the region of the trapezoid body and the ipsilateral and contralateral superior olives). Examination of the fields 100  $\mu$ sec before and after those shown in Fig. 7 revealed movement of the positive potential in the ventral region of the brain stem in a contralateral direction. The distribution and movement of this field followed the course of the fibers in the trapezoid body.

### N2.0

At the latency of N2.0 (Fig. 8) there were 3 major sites of activity. First, there was an 800  $\mu$ V positive field located dorsal and rostral and a 200  $\mu$ V negative field located ventral in the cochlear nucleus. Second, there was another dipole field located at ipsilateral 6 between the cochlear nucleus (plane I8) and the superior olive (plane I4). And third, the positive field located in the ventral region of the brain stem at P1.7 now increased in amplitude to 400–1000  $\mu$ V. The origin of the dipole field at ipsilateral 6 was unclear as

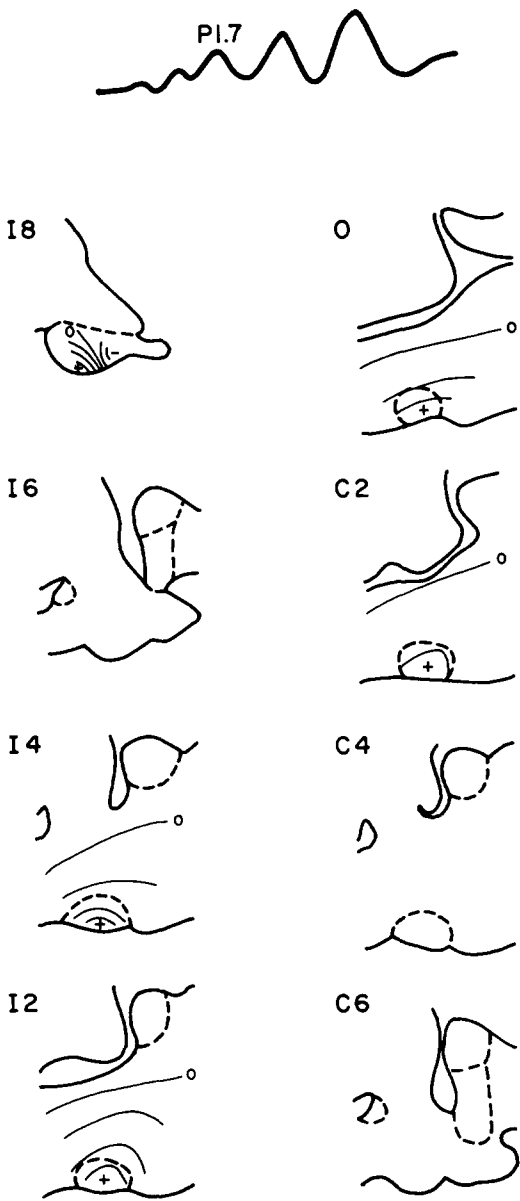


Fig. 7. Spatial distribution of the voltage fields in the brain stem at the latency of component P1.7. A dipole field was located in the cochlear nucleus with the negative pole rostral and dorsal and the positive field caudal and ventral. A positive field was also present in the ventral region of the brain stem from ipsilateral 4 (I4) to contralateral 4 (C4). In this and all subsequent figures the anatomical regions contained within the dashed lines are noted in Fig. 5.

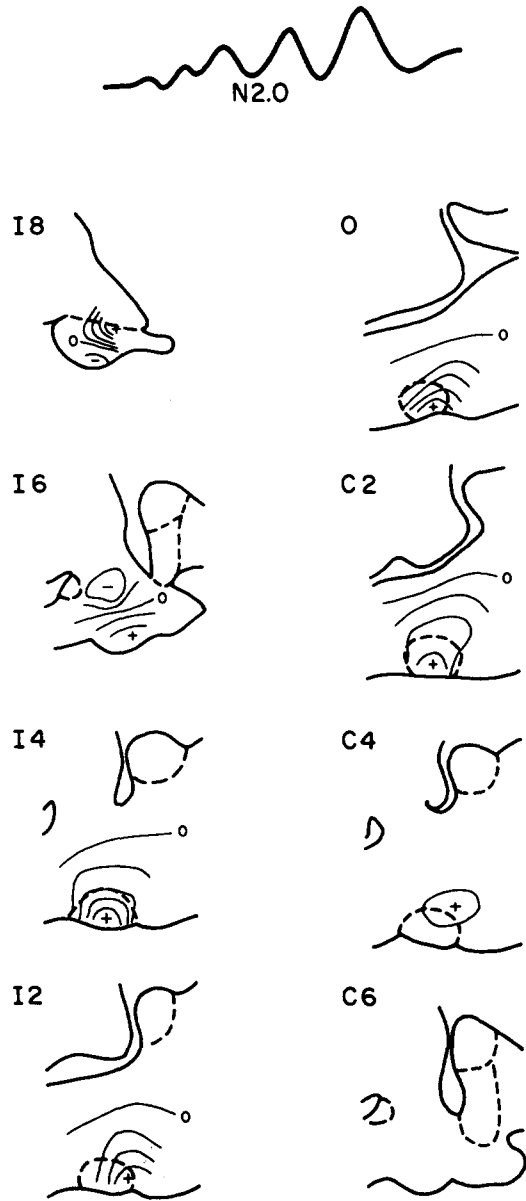


Fig. 8. Spatial distribution of the voltage fields in the brain stem at the latency of component N2.0. In the cochlear nucleus there was an 800  $\mu$ V positive field located dorsal and rostral and a 200  $\mu$ V negative field located ventral. The positive field in the ventral brain stem from ipsilateral 4 to contralateral 4 increased in amplitude as compared with the same field seen at the latency of P1.7.

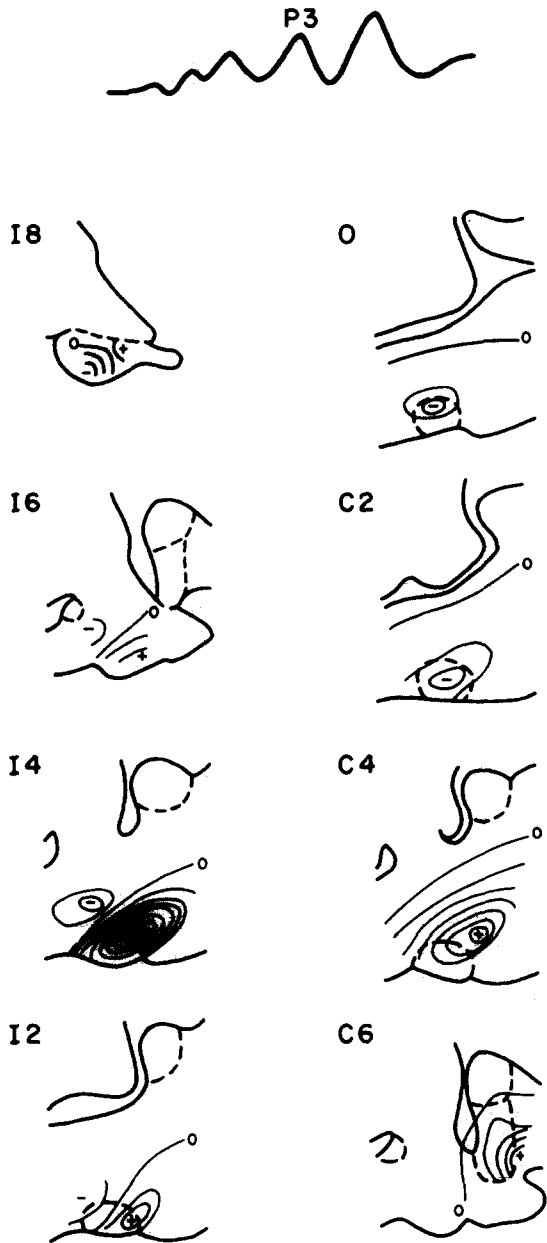


Fig. 9. Spatial distribution of the voltage fields in the brain stem at the latency of component P3. Prominent fields were present in the ipsilateral (plane I4) and contralateral superior olives (plane C4) and in the contralateral lateral lemniscus (plane C6). The field in the ipsilateral superior olive was a dipole with a 1400  $\mu\text{V}$  positive pole located rostral and ventral and a 400  $\mu\text{V}$  negative pole located dorsal and caudal. In the contralateral superior olive there was a 1200  $\mu\text{V}$  positive field which extended into the lateral lemniscus. A

400  $\mu\text{V}$  negative field was also located in the region of the trapezoid body and contralateral superior olive, but it was more medial and ventral.

### P3

At the latency of P3 (Fig. 9) prominent fields were located in the ipsilateral and contralateral superior olives and the contralateral lateral lemniscus. The field in the ipsilateral superior olive (plane I4) was a dipole with a 1400  $\mu\text{V}$  positive pole located rostral and ventral and a 400  $\mu\text{V}$  negative pole located dorsal and caudal. In the contralateral superior olive (plane C4) there was a 1200  $\mu\text{V}$  positive field, which extended into the lateral lemniscus (plane C6). The small negative field at C2 medial and ventral to this positive field suggested that there was either a dipole in the contralateral superior olive or a triphasic compound action potential in the trapezoid body with the leading positivity in the region of the contralateral lateral lemniscus, the negative component in the region of the midline portion of the trapezoid body and the trailing positivity in the region of the ipsilateral superior olive. Fig. 10 contains the plane of section in the region of the contralateral lateral lemniscus (C6) and shows the rapid change of the voltage field over 200  $\mu\text{sec}$ . The voltage field increased in amplitude 6-fold from 200  $\mu\text{V}$  to 1200  $\mu\text{V}$  and moved dorsal over this short time span, suggesting movement of the field up the lateral lemniscus.

### N3

At the latency of N3 prominent fields were located in the ipsilateral superior olive and in the contralateral superior olive and lateral lemniscus (Fig. 11). The large amplitude field in the ipsilateral superior olive present at the latency of P3 diminished with the positive pole decreasing to 1000  $\mu\text{V}$  and the negative pole decreasing to 200  $\mu\text{V}$ . The 1400  $\mu\text{V}$  positive field in the contralateral lateral lemniscus

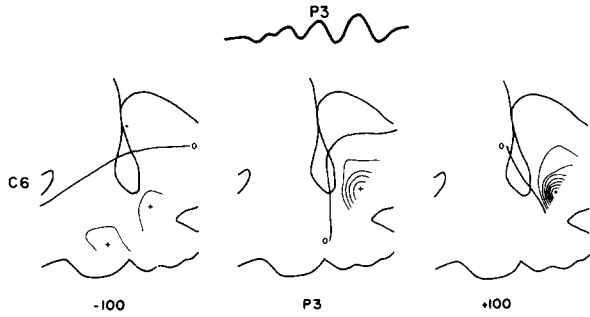


Fig. 10. Temporal distribution of the voltage fields in the contralateral lateral lemniscus at the latency of component P3. Within a span of 200  $\mu$ sec (-100 to +100) the positive field in the lateral lemniscus increased in amplitude from 200  $\mu$ V to 1200  $\mu$ V and the field moved in a dorsal direction.

shown in Fig. 12 increased to 2000  $\mu$ V by 100  $\mu$ sec after the latency of N3.

P4

Fig. 12 depicts the spatial distribution of voltage throughout the brain stem at the latency of P4. Prominent fields were seen in the ipsilateral and contralateral superior olives (planes I4 and C4) and in the contralateral lateral lemniscus (plane C6). The field maps recorded 100  $\mu$ sec before and after the latency of P4 showed movement of the positive pole of the dipole in the ipsilateral superior olive towards the ipsilateral lateral lemniscus and a dorsal movement of the positive field in the contralateral lateral lemniscus towards the inferior colliculus.

N4

At the latency of N4 prominent fields were present in the ipsilateral superior olive (plane I4) and the contralateral superior olive (C4) and lateral lemniscus (C6) (Fig. 13). The largest field (1800  $\mu$ V) was located in the contralateral lateral lemniscus. A small field was also located just ventral to the inferior colliculus and medial to the lateral lemniscus at ipsilateral 4.

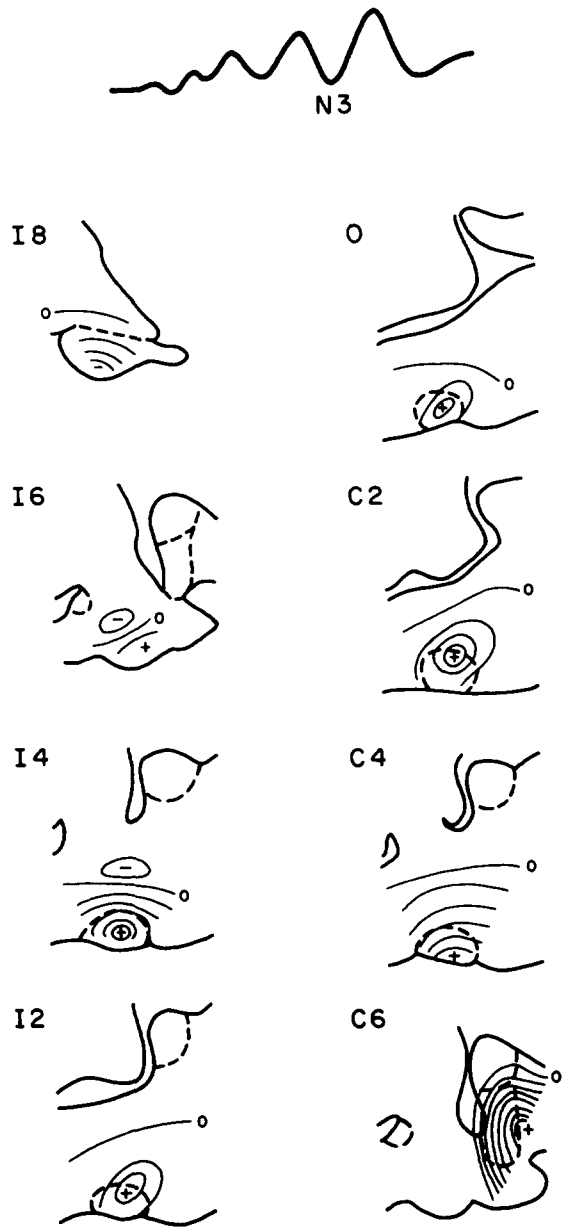


Fig. 11. Spatial distribution of the voltage fields in the brain stem at the latency of component N3. Prominent fields were evident in the ipsilateral superior olive (plane I4) and the contralateral superior olive (plane C4) and lateral lemniscus (plane C6). In comparison to the potentials recorded at the latency of P3 the amplitude of the positive and negative poles of the dipole in the ipsilateral superior olive decreased to 1000 and 200  $\mu$ V, respectively. The field in the contralateral lateral lemniscus increased to 1400  $\mu$ V.

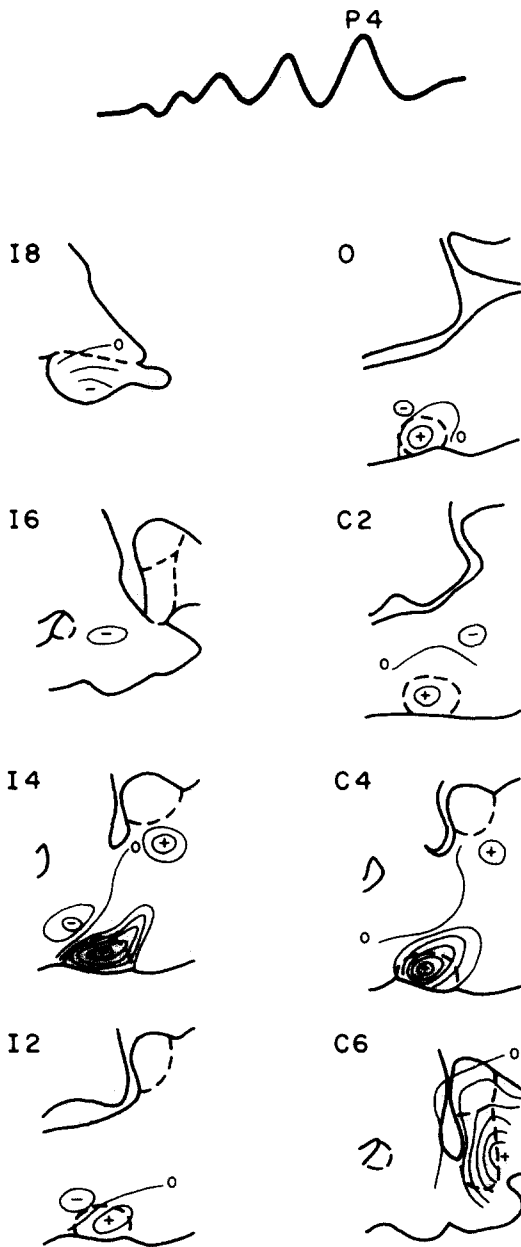


Fig. 12. Spatial distribution of the voltage fields in the brain stem at the latency of component P4. Prominent fields were present at the latency of P4 in the ipsilateral superior olive (plane I4) and the contralateral superior olive (plane C4) and lateral lemniscus (plane C6). The negative pole of the dipole in the ipsilateral superior olive was  $400 \mu\text{V}$  and the positive pole  $1000 \mu\text{V}$ . The  $1000 \mu\text{V}$  positive field in the contralateral lateral lemniscus extended well into the lateral lemniscus.

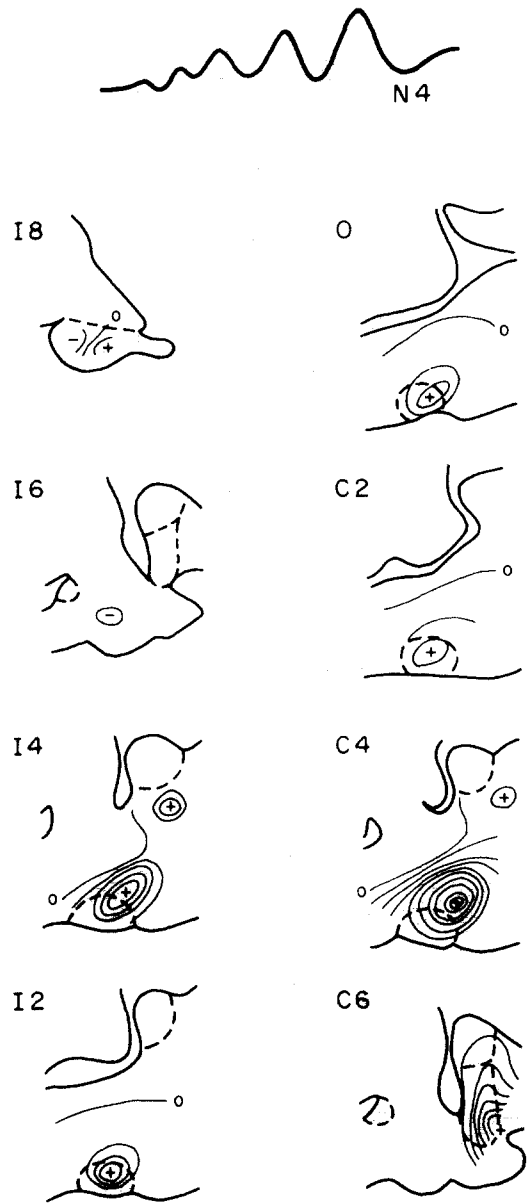


Fig. 13. Spatial distribution of the voltage fields in the brain stem at the latency of component N4. Prominent fields were located in the ipsilateral superior olive (plane I4), in the contralateral superior olive (plane C4) and in the lateral lemniscus (plane C6). The amplitudes of these fields were  $800$ ,  $1800$  and  $800 \mu\text{V}$ , respectively.

*The effects of filtering on the correlation of the spatial and temporal distribution of evoked potentials in the brain stem and the scalp-recorded ABR*

The spatial and temporal distributions of evoked potentials in the brain stem were affected by filtering of the evoked potentials with a bandpass of 160 Hz–3 kHz. The effects were due solely to the attenuation of low frequency activity as no significant changes were found in the evoked potential wave forms when only high frequency components (greater than 3 kHz) were attenuated. The most prominent change found with filtering was a decrease in amplitude of the evoked potentials attributable to the attenuation of low frequency components. In contrast, the ABR recorded from the surface electrode was relatively unaffected by filtering, except for the loss of a slow positive baseline shift beginning at about the latency of component P1.7.

While changes occurred in the magnitude, polarity and orientation of the fields recorded in the brain stem between the unfiltered and filtered conditions, the regions of the brain stem which had prominent activity in the unfiltered condition also had prominent activity in the filtered condition. The only exception was for component P4. Fig. 14 shows the spatial distribution of filtered evoked potentials throughout the brain stem in cat 4 at the latency of P4. This figure is to be compared with Fig. 12. Because the evoked potentials from the different brain regions had differing contributions of low frequency components, the fields were not affected equally by high pass filtering, leading to changes in their relative amplitudes. Thus, for component P4 the cochlear nucleus and the trapezoid body, which had relatively low amplitude fields in the unfiltered condition, were of comparable amplitude in the filtered condition to the fields in the ipsilateral superior olive and the contralateral superior olive and lateral lemniscus.

Similar findings in both the unfiltered and filtered conditions were obtained in cat 3,

whose data was collected and analyzed in the same manner as the data for cat 4.

*The definition of the brain stem generators contributing to the ABR*

As digital and analog filtering (with the bandpasses used in this study) were found to provide comparable data, the analog filtered data from cats 1 and 2 were combined with the digitally filtered data from cats 3 and 4 to obtain a general description of the distribution of evoked potentials within the brain stem at the latencies corresponding to components P0.8 through N4. Components P5 and later were not analyzed because of their poor definition in the 4 cats. For each of the components of the ABR in each of the 4 cats, the amplitude of the field in a given region of the brain stem was expressed as a percentage of the maximum field anywhere in the brain stem at that instant of time at the 3 latencies characterizing each component:  $-100 \mu\text{sec}$ , peak or trough,  $+100 \mu\text{sec}$ . The 'per cent of maximum field' at each auditory site was averaged across the 4 subjects at the 3 instants of time for each component, with positive and negative fields averaged separately (to prevent the mathematical cancellation of data). Because of the small number of cats used, the data from  $100 \mu\text{sec}$  before and after each peak or trough were included with the data at the latency of the peak or trough to reduce the variability which might have occurred due to a single spurious measure. The results of this analysis are summarized in Fig. 15. Note that little activity was recorded in either the ipsilateral or contralateral inferior colliculus at the latencies of components P0.8 through N4. (As the fields occurring at the latencies of components P5 and later were not evaluated, it is not known what contribution the inferior colliculus makes to these later components.) Furthermore, in none of the 4 animals were notable fields found in any brain areas other than the primary auditory pathway.

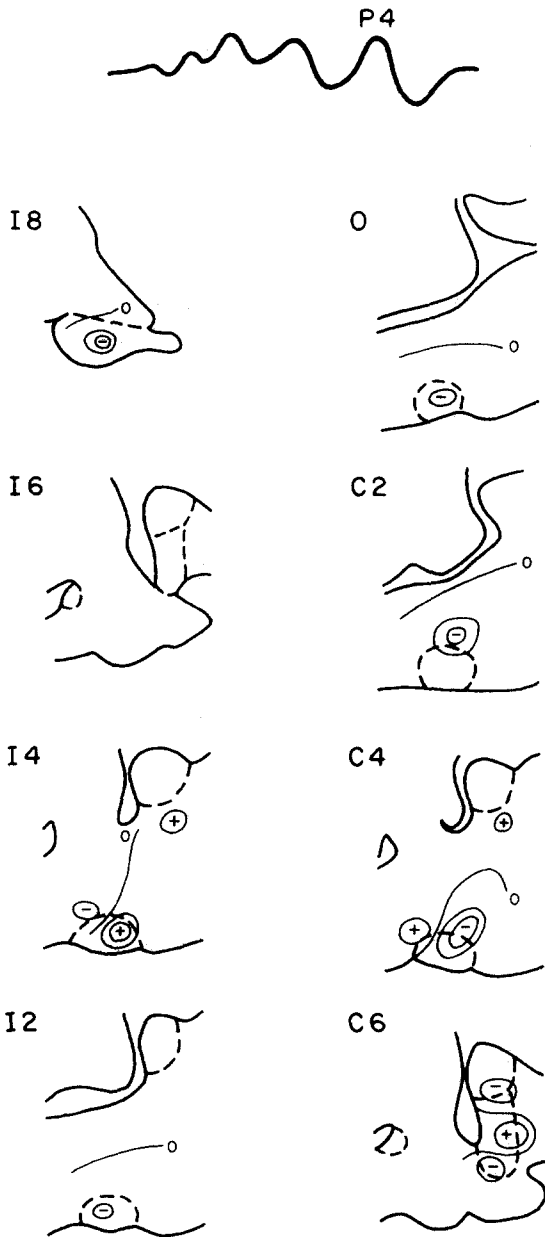


Fig. 14. Spatial distribution of the voltage fields in the brain stem at the latency of component P4 with the amplifier bandpass at 160 Hz–3 kHz. Filtering of the evoked potentials substantially altered the polarity, orientation and absolute magnitudes of the fields in the brain stem at the latency of P4. The spatial distribution of voltage in this figure is to be compared with that in Fig. 12. The sites of substantial evoked activity in the filtered condition were the cochlear nucleus, ipsilateral superior olive, trapezoid body and

Although a number of factors are important in determining the contribution of a field to a distant recording site, a 'generator' was defined as a site whose 'average per cent of maximum field' met or exceeded an arbitrarily defined criterion of 50%. This criterion level minimized the inclusion of brain stem sites with a low level of evoked activity whose contributions to the surface recording were probably insignificant. The degree to which other factors, such as the geometry of the generators, might affect the determination of the generators was not assessed. The generators of the ABR as defined by the above criterion are summarized in Table I. Note that for most of the components two or more brain stem auditory structures satisfied the criterion of an average per cent of maximum field of 50%. The definition of the eighth nerve as the generator of the first 3 components is explained more fully below.

Additional recordings obtained from the round window simultaneously with the scalp-recorded ABR suggested that the first 3 components of the ABR (P0.8, N1.0, and P1.2) were generated by the eighth nerve. The waveform recorded from the round window (Fig. 1, dark trace in bottom pair of traces) consisted of a large negative potential N1, followed by a positive potential and a second smaller negative potential, N2. The first two components of this response (N1 and P1) were shown by Davis et al. (1952) to be closely related to action potentials in the eighth nerve. A triphasic (positive-negative-positive) compound action potential is usually recorded from fiber tracts, but in round window recordings of eighth nerve activity the initial positive component is minimal or absent. Dallos (1973) has shown that the failure to detect the initial positive component is due to the insulating properties of the bone of

the contralateral superior olive and lateral lemniscus. The filtered ABR at the top of the figures is the same as the unfiltered ABR shown in earlier figures, except for the attenuation of the slow positive baseline shift.

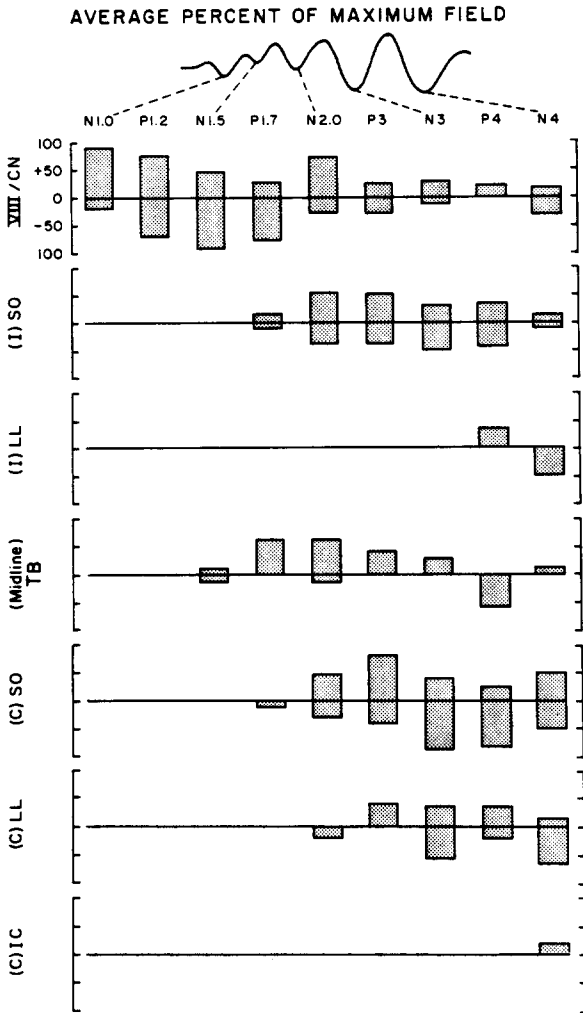


Fig. 15. The amplitude distribution of the voltage fields in the brain stem auditory pathway of the cat at the latencies of the components of the ABR. The data in this figure were derived in two steps. First, for each cat, the amplitude of the field in a given region of the brain was expressed as a percentage of the maximum field anywhere in the brain stem at that instant of time. Second, the findings from the individual analyses of the isopotential maps for the 4 animals were averaged across the 3 instants of time (-100, peak, +100) for each component. The positive and negative fields were averaged separately. The individual components of the ABR are given along the abscissa in this figure. The ordinate for each of the auditory structures at the left margin is the average per cent of maximum field. From 0 to +100 and from 0 to -100 are separate averages. The standard error of the mean varied from 2 to 13 across the compo-

the cochlea. The initial positive component is also absent at the medial side of the internal auditory meatus; however, the potential changes to a triphasic (positive-negative-positive) wave form shortly after the eighth nerve exits from the internal auditory meatus (Mouseghian et al. 1962). In Fig. 1 it can be seen that the time course of N1-P1 of the round window recording was very close to that of P0.8, N1.0 and P1.2 of the ABR. The eighth nerve origin of the early components of the ABR was also suggested by the movement of the potentials from the midventral cochlear nucleus into the region of the anteroventral cochlear nucleus, following the course of the eighth nerve fibers within the cochlear nucleus. It is not known if this sequence of fields also occurred in the posteroventral cochlear nucleus as this area was not adequately sampled in the 4 cats.

### Discussion

The results from this study indicate that except for the first few components of the ABR, which are believed to be generated solely by the eighth nerve, each of the other major components of the ABR can be correlated with substantial activity in two or more auditory structures. This finding obviously questions the current view in the literature that each component of the ABR is primarily due to activity in a single site along the audi-

nents and structures. The recordings were made with the amplifier bandpass set to attenuate low frequency electroencephalographic activity. The abbreviations are: VIII/CN, eighth nerve, cochlear nucleus; SO, superior olive; LL, lateral lemniscus; TB, trapezoid body; IC, inferior colliculus; (I), ipsilateral; (C), contralateral. No data are presented for the ipsilateral inferior colliculus because of the absence of any significant activity through the latency of component N4. The region of the eighth nerve and cochlear nucleus was considered as a single generator, as the individual contributions of these two structures could not be readily distinguished.

TABLE I

Major sites of brain stem activity correlated with the components of the ABR. VIII N., eighth nerve; CN, cochlear nucleus; SO, superior olive; LL, lateral lemniscus; TB, trapezoid body; (I), ipsilateral; (C), contralateral.

	Component									
	P0.8	N1.0	P1.2	N1.5	P1.7	N2.0	P3	N3	P4	N4
VIII N.	*	*	*							
VIII N./CN				*	*	*				
(I)SO						*	*	*	*	
(I)LL										*
TB					*	*			*	
(C)SO						*	*	*	*	*
(C)LL								*	*	*

tory pathway. Moreover, for certain components there were several important distinctions between the findings in the present study, employing a map of the distribution of potentials in the brain stem, and those from previous studies in which lesions were made in the brain stem auditory pathway. First, in the present study substantial activity was defined in the trapezoid body and the cochlear nucleus at the latency of P1.7. This is inconsistent with the finding by Buchwald and Huang (1975) that isolation of the cochlear nucleus from the rest of the brain stem had no effect on this component. One possibility which may account for this discrepancy is that component P1.7 when recorded from the vertex referenced to the pinna, as in the study by Buchwald and Huang, might have a much smaller proportion of volume-conducted activity from the trapezoid body than when recorded from the frontal sinus referenced to the neck as in the present study. Thus, destruction of the trapezoid body would have less effect on P1.7 when the ABR is recorded from the vertex referenced to the pinna.

A second discrepancy between the results of the present study and the effects of brain stem lesions on the ABR is the finding of substantial activity in the ipsilateral superior olivary complex at P3. Buchwald and Huang (1975) concluded that P3 was largely dependent upon contralateral structures, since this

component was lost following hemisection of the brain stem. There are, however, several mechanisms that might account for the change in P3 or in any evoked potential component following a lesion. The evoked potential may be altered because (1) the lesioned structure was indeed the generator of the component; (2) there was damage to fibers passing through the lesioned structure which connect to the actual generator located some distance away; (3) there were physiological disturbances to the generator located in a region remote from the lesion due to circulatory or pressure effects; and (4) the lesion resulted in altered function of the remaining neural elements. As an example of the last mechanism, several investigators (Patton 1965; Dallos 1973; Schlag 1973) have demonstrated that acute section of a fiber tract (such as the trapezoid body) alters the normal triphasic compound action potential recorded from the fiber tract to a monophasic negative potential at the point of destruction of the tract. A distant electrode would record a triphasic wave form from the intact portion of the fiber tract and a monophasic negative potential from the severed end. Thus, the loss of P3 following the transection of the trapezoid body could be due to altered potentials generated by the remaining structures rather than to the loss of input to contralateral structures.

A surprising finding in the present study was that little activity was present in the inferior colliculus at the latency of component P4. The voltage fields that were recorded from the vicinity of the inferior colliculus were of relatively low amplitude and were volume-conducted from adjacent portions of the lateral lemniscus. This result is discrepant from the findings of Jewett (1970) and Lev and Sohmer (1972) that the region of the inferior colliculus was the most active site in the brain stem at the latency of component P4. The finding in the present study that the inferior colliculus does not contribute substantially to component P4 is supported by the absence of an effect on component P4 with lesions destroying the input to the inferior colliculus (Buchwald and Huang 1975).

The analysis of filtering effects on the distribution of field potentials in the brain stem and their correlation with the components of the ABR indicates that while dramatic changes may occur in the orientation or absolute magnitude of the fields as a function of filtering, the apparent relative contributions of the brain stem auditory sites show only modest change. In only one instance (component P4) did the changes in the apparent relative contributions result in a different defined set of generators. This suggests that within the range of filter settings employed in this study, filtering has a minimal influence on the determination of the generators of the components of the ABR, as defined by the spatial and temporal development of evoked potentials in the brain stem.

The results in the present study provide no consistent relationship between the polarities of the maximum fields in the brain stem and the polarity of the surface recorded components of the ABR. In many instances the polarity of a given component of the ABR was opposite to the polarity of the dominant field(s) in the brain stem. In studies by Jewett (1970) and Lev and Sohmer (1972) a large amplitude, negative-going wave recorded with an intracranial electrode was taken as evidence that the wave was generated at the elec-

trode site and a large amplitude positive wave was taken as evidence of activity progressing in a volume conductor along the classical ascending auditory pathway towards the surface. While there is a possibility that these criteria might be correct for all of the components of the ABR, other alternatives exist. Inasmuch as a given field potential depends, at a minimum, on the geometrical shapes of the sinks and sources of current, the distance between the sinks and sources, and their relative magnitudes (Humphrey 1968), it is difficult to arrive at a satisfactory criterion for correlating the polarity of the potentials seen in the brain stem with those at the surface. It is likewise difficult to arrive at a satisfactory criterion for correlating the amplitude of the potentials at the surface and in the brain stem, as in the present study. Thus, although this study documents the complexity of the spatial and temporal distribution of auditory evoked potentials within the brain stem at the latencies of the components of the ABR, a solution is needed for defining how these potentials interact to generate the far-field ABR recorded on the scalp.

The major sites of significant activity listed in Table I provide a set of possible major generators for the components of the ABR. Even though this study did not provide any information on how these major sites of activity sum at the surface, the definition of significant activity in widespread areas of the brain stem at the time of occurrence of several components of the scalp-derived ABR suggests that the concept of a simple one-to-one relationship between a given component of the ABR and a single auditory structure is unlikely. Moreover, the designation of a single auditory structure as the primary contributor to a given component is also tenuous.

## Summary

A spatial and temporal analysis of auditory evoked potentials within the brain stem were performed in cats to determine the areas of

the brain stem having large amplitude voltage fields, corresponding in latency to each of the components of the scalp-recorded auditory brain stem response (ABR). On the basis of this criterion, the first few components (occurring within 2 msec post-stimulus) were attributed to activity in a single structure, the eighth nerve. In contrast, each of the other components was correlated with large amplitude fields in at least two sites within the brain stem auditory pathways. The findings demonstrate a complex spatial and temporal distribution of electrical events within the auditory brain stem pathways, which preclude any simple one-to-one relationship between a given anatomical site and a particular component of the ABR.

The possibility that the determination of the generators might be influenced by filtering of the evoked potentials was also examined. High-pass filtering of the evoked potentials resulted in a modification of the defined generators for only one of the components studied (P4). Filtering had little effect on the components of the scalp-recorded ABR.

## Résumé

### *Réponses auditives du tronc cérébral chez le chat. I. Enregistrements intracrâniens et extracrâniens*

Une analyse spatiale et temporelle des potentiels évoqués auditifs à l'intérieur du tronc cérébral a été réalisée chez le chat pour déterminer les régions du tronc cérébral qui ont des champs de grand voltage, dont la latence correspond à chacune des composantes de la réponse auditive du tronc cérébral (ABR) enregistrée sur le scalp. Sur la base de ce critère, les quelques premières composantes (survenant dans les 2 msec post-stimulus) sont attribuées à l'activité d'une seule structure, le nerf auditif. Par contraste, chacune des autres composantes est corrélée avec des champs de grande amplitude dans au moins deux régions à l'intérieur des voies auditives du tronc céré-

bral. Ces données démontrent une distribution spatiale et temporelle complexe des événements électriques à l'intérieur des voies auditives du tronc cérébral, qui infirment toute relation simple et ponctuelle entre un lieu anatomique donné et une composante particulière du ABR.

La possibilité que la détermination des générateurs puisse être influencée par le filtrage des potentiels évoqués a été également étudiée. Un filtrage passe-haut des potentiels évoqués résulte en une modification des générateurs définis pour seulement une des composantes étudiées (P4). Le filtrage a peu d'effet sur les composantes du ABR enregistré sur le scalp.

## References

- Achor, L.J. and Starr, A. Auditory brain stem responses in the cat. II. Effects of lesions. *Electroenceph. clin. Neurophysiol.*, 1980, 48: 174-190.
- Berry, H., Blair, R.L., Bilbao, J. and Briant, T.D.R. Click evoked eighth nerve and brain stem responses (electrocochleogram) — experimental observations in the cat. *J. Otol.*, 1976, 5: 64-73.
- Brigham, E. *The Fast Fourier Transform*. Prentice-Hall, Englewood Cliffs, N.J., 1974.
- Buchwald, J.S. and Huang, C.-M. Far-field acoustic responses: origins in the cat. *Science*, 1975, 189: 382-384.
- Dallos, P. *The Auditory Periphery*. Biophysics and Physiology. Academic Press, New York, 1973.
- Davis, H., Tasaki, I. and Goldstein, R. The peripheral origin of activity, with reference to the ear. *Cold Spr. Harb. Symp. quant. Biol.*, 1952, 17: 143-154.
- Goldenberg, R.A. and Derbyshire, A.J. Averaged evoked potentials in cats with lesions of auditory pathway. *J. Speech Res.*, 1975, 18: 420-429.
- Humphrey, D.R. Re-analysis of the antidromic cortical response. II. On the contribution of cell discharge and PSPs to the evoked potentials. *Electroenceph. clin. Neurophysiol.*, 1968, 25: 421-442.
- Jewett, D.L. Averaged volume-conducted potentials to auditory stimuli in the cat. *Electroenceph. clin. Neurophysiol.*, 1970, 28: 609-618.
- Jewett, D.L. and Williston, J.S. Auditory evoked far fields averaged from the scalps of humans. *Brain*, 1971, 94: 681-696.
- Jungert, S. Auditory pathways in the brainstem. *Acta otolaryng. (Stockh.)*, 1958, Suppl. 138: 1-67.

- Lev, A. and Sohmer, H. Sources of averaged neural responses recorded in animal and human subjects during cochlear audiometry (electrocochleography). *Arch. klin. exp. Ohr-, Nas-, u. Kehlk.-Heilk.*, 1972, 201: 79-90.
- Mouseghian, G., Rupert, A. and Galambos, R. Micro-electrode study of the ventral cochlear nucleus of the cat. *J. Neurophysiol.*, 1962, 25: 515-529.
- Patton, H.D., Special properties of nerve trunks and tracts. In: T.C. Ruch and H.D. Patton (Eds.), *Neurophysiology*, 2nd edition. Saunders, Philadelphia, Pa., 1965: 73-94.
- Schlag, J. Generation of brain evoked potentials. In: R.F. Thompson and M.M. Patterson (Eds.), *Bioelectric Recording Techniques, Part A*. Academic Press, New York, 1973: 273-316.
- Starr, A. and Achor, L.J. Auditory brain stem responses in neurological disease. *Arch. Neurol.* (Chic.), 1975, 32: 761-768.
- Stockard, J.J. and Rossiter, V.S. Clinical and pathological correlates of brain stem auditory response abnormalities. *Neurology (Minneapolis)*, 1977, 27: 316-325.
- Terkildsen, K., Osterhammel, P. and Huis in't Veld, F. Electrocochleography with a far field technique. *Scand. Audiol.*, 1973, 2: 141-148.
- Thornton, A.R.D. and Hawkes, C.H. Neurological applications of surface recorded electrocochleography. *J. Neurol. Neurosurg. Psychiat.*, 1976, 39: 586-592.
- Wicklegren, W.O. Effects of state of arousal on click-evoked responses in cats. *J. Neurophysiol.*, 1968, 31: 757-768.
- Williston, J.S. and Jewett, D.L. The  $Q_{10}$  of auditory brainstem responses in rats under hypothermia. *Soc. Neurosci., 7th Ann. Meeting*, 1977: 134.